HHS Public Access

Author manuscript

ChemPhotoChem. Author manuscript; available in PMC 2017 October 16.

Published in final edited form as:

ChemPhotoChem. 2017 March ; 1(3): 89–92. doi:10.1002/cptc.201600044.

Intramolecular Photogeneration of a Tyrosine Radical in a Designed Protein

Alison G. Tebo[b], **Annamaria Quaranta**[c], **Christian Herrero**[a], **Vincent L. Pecoraro**[b], and **Ally Aukauloo**[a,c]

[a]Dr. C. Herrero, Prof. A. Aukauloo, Institut de Chimie Moléculaire et des Matériaux D'Orsay, Université Paris Sud, Université Paris Saclay, CNRS UMR 8182, 91405 Orsay Cedex (France)

[b]Dr. A. G. Tebo, Prof. V. L. Pecoraro, Department of Chemistry, University of Michigan, Ann Arbor, MI 48109 (USA)

[c]Dr. A. Quaranta, Prof. A. Aukauloo, CEA Saclay, iBiTecS, Service de Bioénergétique Biologie Structurale et Mécanismes (SB_2SM), Gif-sur-Yvette, 91191 (France)

Abstract

Long-distance biological electron transfer occurs through a hopping mechanism and often involves tyrosine as a high potential intermediate, for example in the early charge separation steps during photosynthesis. Protein design allows for the development of minimal systems to study the underlying principles of complex systems. Herein, we report the development of the first ruthenium-linked designed protein for the photogeneration of a tyrosine radical by intramolecular electron transfer.

Keywords

electron transfer; photochemistry; protein design; radicals; tyrosine

Electron transfer (ET) is an important process that plays key roles in sustaining life through photosynthesis and respiration as well as in the development of new technologies for green energy. Biological ET must often occur over large distances (≈ 30 Å) with a sufficiently high rate to sustain life.[1] Long-distance electron transfer proceeds by a series of hops, which reduces the distance dependence of the rate of ET.[2–4] The protein matrix itself can be involved in mediating ET directly through the participation of redox-active amino acids, such as tyrosine and tryptophan.[5]

Stable amino acid based radicals are recognized as essential components of both electron transfer and catalytic processes in many proteins that can play both oxidative and reductive roles, as their reduction potentials are highly sensitive to their protonation state and chemical environment.[6] In particular, tyrosine radicals are vital to long-distance ET in many important biological systems, such as photosystem II (PSII), ribonucleotide reductase

Supporting information and the ORCID identification number(s) for the author(s) of this article can be found under: http ://dx.doi.org/10.1002/cptc.201600044.

(RNR), and cytochrome c oxidase.[1] Tyrosine radical chemistry in biological processes is complicated by the fact that acid-base chemistry is coupled to electron transfer, which results from the difference in pK_a values between neutral tyrosine (pK_a = 10) and the tyrosyl radical (pK_a = −2).[7] Thus, over the physiologically relevant pH range, proton-coupled electron transfer (PCET) occurs. Since tyrosine undergoes a PCET process, tyrosines in native proteins are often hydrogen bonded to nearby amino acids and water molecules, facilitating fast reactions by providing nearby proton acceptors.[8] Although the importance of tyrosine radicals in natural processes is well known, the details of their behavior is challenging to study because of the complexity of the systems of which they are a part. Moreover, understanding their role in vectorial electron transfer may help chemists to employ similar functionalities in the design of bioinspired materials.

Previously, amino acid based radicals had been studied by spectroscopic characterization of mutants and perturbed forms of native proteins.[5,9,10] Engineered forms of azurin and RNR have been used to study tyrosine radicals in native proteins.[11–13] More recently, scientists have turned to protein design as a method to create systems with sufficient complexity to understand the basics of functionality in native systems, while retaining a high degree of control over the system. A single tyrosine in a de novo designed α-helical bundle was recently reported and was characterized by electrochemistry[14] and transient absorption spectroscopy.[15] This tyrosine radical was extremely stable and exhibited long lifetimes as a result of the fact that it is buried in the hydrophobic interior of the protein. As radicals are typically intermediate electron relays in intramolecular electron-transfer reactions, some synthetic systems have been developed to mimic tyrosine-based relays.[16,17] However, further work is needed to better understand the roles and mechanisms inherent to protein-based tyrosines.

By using de novo protein design methods, we sought to develop a system to generate and study tyrosine radical involvement in intramolecular electron transfer. Our lab has previously reported de novo designed α-helical bundles for modeling metal binding sites, hydrolytic and redox catalysis, and electron transfer.[18–24] These proteins are designed to mimic globular proteins and exhibit a well-folded and characterized tertiary structure. We hypothesized that a variant form of the peptide α_3DH_3, which was previously characterized for hydrolytic activity,[21] would be an excellent scaffold for controlled studies on intramolecular electron transfer in proteins via tyrosine radicals. Replacing the terminal residue with a cysteine generated a site useful for the covalent attachment of chromophores within the electron-transfer distance of Tyr70, which is located at the interface between two helices (Figure 1 A). In this study, we have not optimised and studied the chemical environment of the tyrosine motif that can be tuned by its position on the protein scaffold. Such a systematic study is beyond the scope of this preliminary communication and will be addressed in future work.

Ruthenium trisbipyridine $[Ru^{II}(bpy)_3]^{2+}$ compounds and their derivatives are well-characterized and widely used photosensitizers with a long-lived triplet excited state that has the capacity to either accept or donate one electron.[25,26] These characteristics have led to the widespread use of $[Ru^{II}(bpy)_3]^{2+}$ analogues to trigger and understand photoinduced catalytic and electron-transfer reactions.[25] Previous studies on $[Ru^{II}(bpy)_3]^{2+}$ derivatives

showed that functionalization of the bipyridines with a triazole ring resulting from the copper-catalyzed azide-alkyne addition reaction does not significantly alter the characteristics of this excited state.[27,28] Further photophysical studies showed that the triazole linkage can efficiently mediate electron transfer from the $[Ru^{II*}(bpy)_3]^{2+}$ either to an electron acceptor or an electron donor.[28] Hence, we reasoned that modifying the bipyridine ligand through click chemistry to introduce a maleimide moiety should not affect the photophysical properties of the lumophore. Inspired by this prior work, we have developed a $[Ru^{II}(bpy)_3]^{2+}$ derivative (**Rubpymal**) that can be appended to free cysteine residues (Figure 1 A; see also Scheme S1 in the Supporting Information). This was used to modify α_3DH_3 selectively at position 75 to give α_3DH_3-**Rubpymal**. These studies provide a proof-of-principle for being able to design complex systems involving separate redox sites that must communicate over long distances. We present a designed system that examines ET properties of a solvent-exposed tyrosine. The combination of a new chromophore for protein labelling with a scaffold for the systematic alteration of protein- or metal-based redox co-factors provides an attractive platform to generate and characterize tyrosine radicals produced by photoinduced electron transfer. More importantly, this protein system represents a foundation for the development of artificial electron-transfer conduits based on α-helical bundles.

Rubpymal was synthesized (see the Supporting Information) and conjugated to α_3DH_3 by reaction of the thiol of Cys75 with the maleimide moiety. After purification, the successful formation of α_3DH_3-Rubpymal was confirmed by QTOF-MS. The estimated distance between the ruthenium and the tyrosine is about 16 Å, based on the solution structure of a related pep- tide[22] and the sizes of the triazole and ruthenium trisbipyridine units.[29] The ground-state absorption spectrum of α_3DH_3-Rubpymal exhibits a typical metal-to-ligand charge transfer (MLCT) band for ruthenium trisbipyridine-based chromophores (Figure S1). The emission spectrum band maximum is located at $\lambda = 640$ nm, in agreement with $Ru(bpy)_3$-triazole derivatives previously investigated.[28] The excited-state lifetime in α_3DH_3-**Rubpymal** was halved ($\tau \approx 400$ ns) compared to Ru-triazole, suggesting that some interaction between the peptide and the chromophore may take place in the excited state. However, the nanosecond transient absorption spectrum shows features typical of triazole functionalization (Figure S2).

Nanosecond laser flash photolysis was used to investigate the electron-transfer reactions and kinetics of the covalently linked ruthenium-peptide adduct (α_3DH_3-**Rubpymal**). Ruthenium hexaamine $[(Ru^{III}(NH_3)_6)]^{3+}$ was used as a reversible electron acceptor to generate the oxidized form of the photoactive unit, for example, $[\mathbf{Ru^{III}bpymal}]^{3+}$, which could then, in turn, oxidize Tyr70. Upon irradiation into the MLCT of $[\mathbf{Ru^{II}bpymal}]^{2+}$, traces were collected at wavelengths of interest to characterize the kinetics of the observed process. Experiments on α_3DH_3-**Rubpymal** resulted in traces with three kinetic regimes (Figure 2A). By comparing control experiments with only $[Ru^{II}(bpy)_3]^{2+}$ and $[Ru^{III}(NH_3)_6]^{3+}$ in solution, the fastest kinetic step ($\tau = 40$ ns, $k_q = 1.1 \times 10^9 m^{-1}s^{-1}$; where k_q is the quenching rate constant) was identified as an intermolecular electron transfer from the excited state of the chromophore to $[Ru^{III}(NH_3)_6]^{3+}$ to generate α_3DH_3-$[\mathbf{Ru^{III}bpymal}]^{3+}$ (Figure 2B, inset). This step is independent of the subsequent reactions involving the generated Ru^{III} species

and is present in all spectra collected. The photogenerated [**Ru^{III}bpymal**]$^{3+}$ was characterized by the depletion of the MLCT band at 450 nm and possesses a high oxidizing power with a reduction potential (E_o) for the $Ru^{3+/2+}$ couple measuring circa 1.2 V vs. NHE.[25,27,28] The second kinetic phase was associated with an increase in absorption between 360 nm and 420 nm, with maxima at 390 nm and 410 nm, which is typical of a tyrosine radical (Figure 2B). Traces at multiple wavelengths were used to reconstruct the transient absorption spectrum of the tyrosine radical (Figure 2B), which agrees with previously observed tyrosyl radical spectra[13,15,30] and supports the model that reduction of [**Ru^{III}bpymal**]$^{3+}$ occurs by means of electron transfer from Tyr70. A global fit (Scheme 1; see also the Supporting Information) at wavelengths associated with the tyrosine radical found that the intramolecular electron-transfer rate (k_{iet}) from tyrosine to [**Ru^{III}bpymal**]$^{3+}$ is circa $3.3 \times 10^5 s^{-1}$. This k_{iet} value is consistent with the expected rate constant for electron transfer at 16 Å, based on a simplified model of electron tunneling in proteins.[31] Using $\Delta\varepsilon_{410}$= 3000 m^{-1} cm^{-1}[30] and $\Delta\varepsilon_{410}$ ≈4500 m^{-1} cm^{-1} for Ru^{III} (where ε is the molar extinction coefficient),[26] about 0.9 μm tyrosine radical is produced from 1.4 μM α_3DH_3-[**Ru^{III}bpymal**]$^{3+}$, corresponding to a yield of approximately 60% for the electron transfer from tyrosine to α_3DH_3-[**Ru^{III}bpymal**]$^{3+}$. The third kinetic phase observed corresponds to recombination of the tyrosine radical and $[Ru^{III}(NH_3)_6]^{3+}$ (τ = 210 μs) to return the system to the ground state.

The generation of a tyrosyl radical is tightly linked to intricate electron- and proton-coupled processes. In α_3DH_3-**Rubpymal**, the k_{iet} value is four times faster at pH 9.5 as compared to pH 5.0 (Figure 3), which is consistent with PCET mechanisms in which proton transfer forms part of the rate-limiting step. The yield (≈60%) of tyrosyl radical formation did not change over the range of pH values tested, although the decay became four times faster with increasing pH values. Although the pH dependence of the rate of tyrosine oxidation is not in and of itself enough to assign a mechanism to this process, this system can form the basis of a series of studies to understand protein-based PCET processes through the introduction of hydrogen-bond donors. By studying the effects of these modifications and the extent to which they may perturb the PCET process, we may be able to understand how one mechanism is “chosen” over another.

We performed X-band EPR experiments to confirm the production of a tyrosine radical. In the presence of the nonreversible electron acceptor $[Co^{III}(NH_3)_5Cl]^{2+}$, illumination for 1 min at λ= 460 nm produces a characteristic spectrum of high-spin $[Co^{II}(H_2O)_6]^{2+}$ with a g value of 4.44 and an organic radical (Figure 4A). Closer examination of the organic radical reveals a broad signal centered at g_{iso} = 2.0052, which is typical of a deprotonated tyrosine radical. The spectrum of the radical species between 10 and 60 K is shown in Figure 4B. The EPR spectrum of tyrosine is very sensitive to the conformation and environment of the radical; depending on the angle of rotation, up to six hydrogen atoms can contribute to the hyperfine structure. The radical observed in this system is consistent with other previously observed tyrosine radicals in native proteins[32–34] and thus confirms that this construct is a good model for tyrosine radicals in native proteins.

Given the importance of protein radicals and the complexity of the processes in which they function, simplified model systems can help elucidate the key aspects for function. This

system represents the first de novo designed system for phototriggered intramolecular tyrosine radical formation and is an important tool for exploring the behavior of tyrosine radicals. The similarity to fundamental processes occurring in proteins such as PSII and the ability to selectively modify the protein suggest a departure point for systematic studies. Such a system may be used to explore the requirements for PCET mechanisms, the effect of nearby hydrogen-bonding residues, and the distance dependence of electron-transfer relays. The insertion of a coordinating site to bind a redox-active transition metal ion will provide an alternative way to study the role of redox-active amino acids in charge accumulation at a catalytic site. Furthermore, this study also stands as a first incursion in the de novo design of redox-active proteins and also lays the groundwork for the development of bio-inspired, fully artificial energy-harvesting systems.

Supplementary Material

Refer to Web version on PubMed Central for supplementary material.

Acknowledgments

A.G.T. acknowledges training grant support from the University of Michigan Chemistry-Biology Interface (CBI) training program (NIH grant 5T32GM008597) as well as support from the Chateaubriand Fellowship. V.L.P would like to thank the National Institutes of Health (NIH) for financial support for this research (ES012236). This work was supported in part by the French Infrastructure for Integrated Structural Biology (FRISBI) ANR-10-INSB-05-01 and Labex CHARMMAT

References

1. Dempsey JL, Winkler JR, Gray HB. Chem Rev. 2010; 110:7024–7039. [PubMed: 21082865]
2. Gray HB, Winkler JR. Chem Phys Lett. 2009; 483:1–9. [PubMed: 20161522]
3. Gray HB, Winkler JR. Quart Rev Biophys. 2003; 36:341–372.
4. Moser CC, Keske JM, Warncke K, Farid RS, Dutton PL. Nature. 1992; 355:796–802. [PubMed: 1311417]
5. Barry BA. J Photochem Photobiol B. 2011; 104:60–71. [PubMed: 21419640]
6. Rappaport F, Diner BA. Coord Chem Rev. 2008; 252:259–272.
7. Dixon WT, Murphy D. J Chem Soc Faraday Trans 2. 1976; 72:1221–1230.
8. Umena Y, Kawakami K, Shen J-R, Kamiya N. Nature. 2011; 473:55–60. [PubMed: 21499260]
9. Barry BA. BBA—Bioenergetics. 2015; 1847:46–54. [PubMed: 25260243]
10. Migliore A, Polizzi NF, Therien MJ, Beratan DN. Chem Rev. 2014; 114:3381–3465. [PubMed: 24684625]
11. Di Bilio AJ, Crane BR, Wehbi WA, Kiser CN, Abu-Omar MM, Carlos RM, Richards JH, Winkler JR, Gray HB. J Am Chem Soc. 2001; 123:3181–3182. [PubMed: 11457048]
12. Shafaat HS, Griese JJ, Pantazis DA, Roos K, Andersson CS, Po-pović-Bijelić A, Gräslund A, Siegbahn PEM, Neese F, Lubitz W, Högbom M, Cox N. J Am Chem Soc. 2014; 136:13399–13409. [PubMed: 25153930]
13. Pizano AA, Lutterman DA, Holder PG, Teets TS, Stubbe J, Nocera DG. Proc Natl Acad Sci USA. 2012; 109:39–43. [PubMed: 22171005]
14. Berry BW, Martínez-Rivera MC, Tommos C. Proc Natl Acad Sci USA. 2012; 109:9739–9743. [PubMed: 22675121]
15. Glover SD, Jorge C, Liang L, Valentine KG, Hammarström L, Tommos C. J Am Chem Soc. 2014; 136:14039–14051. [PubMed: 25121576]
16. Moore GF, Hambourger M, Gervaldo M, Poluektov OG, Rajh T, Gust D, Moore TA, Moore AL. J Am Chem Soc. 2008; 130:10466–10467. [PubMed: 18642819]

17. Megiatto JD Jr, Méndez-Hernández DD, Tejeda-Ferrari ME, Teillout A-L, Llansola-Portolés MJ, Kodis G, Poluektov OG, Rajh T, Mujica V, Groy TL, Gust D, Moore TA, Moore AL. Nat Chem. 2014; 6:423–428. [PubMed: 24755594]
18. Chakraborty S, Kravitz JY, Thulstrup PW, Hemmingsen L, DeGrado WF, Pecoraro VL. Angew Chem Int Ed. 2011; 50:2049–2053.Angew Chem. 2011; 123:2097–2101.
19. Tegoni M, Yu F, Bersellini M, Penner-Hahn JE, Pecoraro VL. Proc Natl Acad Sci USA. 2012; 109:21234–21239. [PubMed: 23236170]
20. Yu F, Penner-Hahn JE, Pecoraro VL. J Am Chem Soc. 2013; 135:18096–18107. [PubMed: 24182361]
21. Cangelosi VM, Deb A, Penner-Hahn JE, Pecoraro VL. Angew Chem Int Ed. 2014; 53:7900–7903.Angew Chem. 2014; 126:8034–8037.
22. Plegaria JS, Dzul SP, Zuiderweg ERP, Stemmler TL, Pecoraro VL. Biochemistry. 2015; 54:2858–2873. [PubMed: 25790102]
23. Plegaria JS, Herrero C, Quaranta A, Pecoraro VL. BBA—Bioenergetics. 2016; 1857:522–530. [PubMed: 26427552]
24. Tebo AG, Hemmingsen L, Pecoraro VL. Metallomics. 2015; 7:1555–1561. [PubMed: 26503746]
25. Campagna S, Puntoriero F, Nastasi F, Bergamini G, Balzani V. Top Curr Chem. 2007; 280:117–214.
26. Kalyanasundaram K. Coord Chem Rev. 1982; 46:159–244.
27. Baron A, Herrero C, Quaranta A, Charlot MF, Leibl W, Vauzeilles B, Aukauloo A. Inorg Chem. 2012; 51:5985–5987. [PubMed: 22590981]
28. Baron A, Herrero C, Quaranta A, Charlot MF, Leibl W, Vauzeilles B, Aukauloo A. Chem Commun. 2011; 47:11011–11013.
29. Harrowfield JM, Sobolev AN. Aust J Chem. 1994; 47:763–767.
30. Candeias LP, Turconi S, Nugent J. Biochim Biophys Acta Bioenerg. 1998; 1363:1–5.
31. Moser CC, Dutton PL. Biochim Biophys Acta Bioenerg. 1992; 1101:171–176.
32. Miner KD, Pfister TD, Hosseinzadeh P, Karaduman N, Donald LJ, Loewen PC, Lu Y, Ivancich A. Biochemistry. 2014; 53:3781–3789. [PubMed: 24901481]
33. Allen JP, Kalman L, LoBrutto R, Williams JC. Nature. 1999; 402:696–699.
34. Ma C, Barry BA. Biophys J. 1996; 71:1961–1972. [PubMed: 8889170]

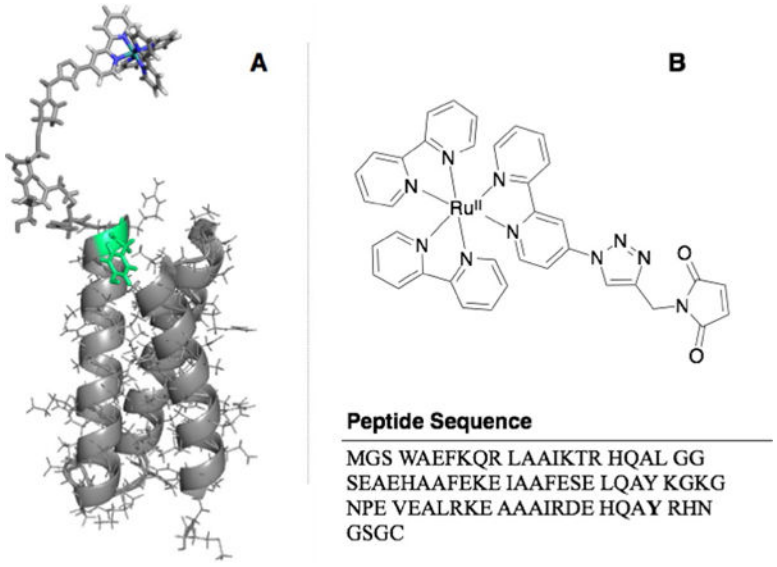

Figure 1.

A) Schematic representation of the structure of α_3DH_3-**Rubpymal** based on the solution NMR structure of a closely related scaffold (PDB: 2MTQ). The key tyrosine residue is marked in green. B) Chemical structure of **Rubpymal** (top) and sequence of α_3DH_3 (bottom).

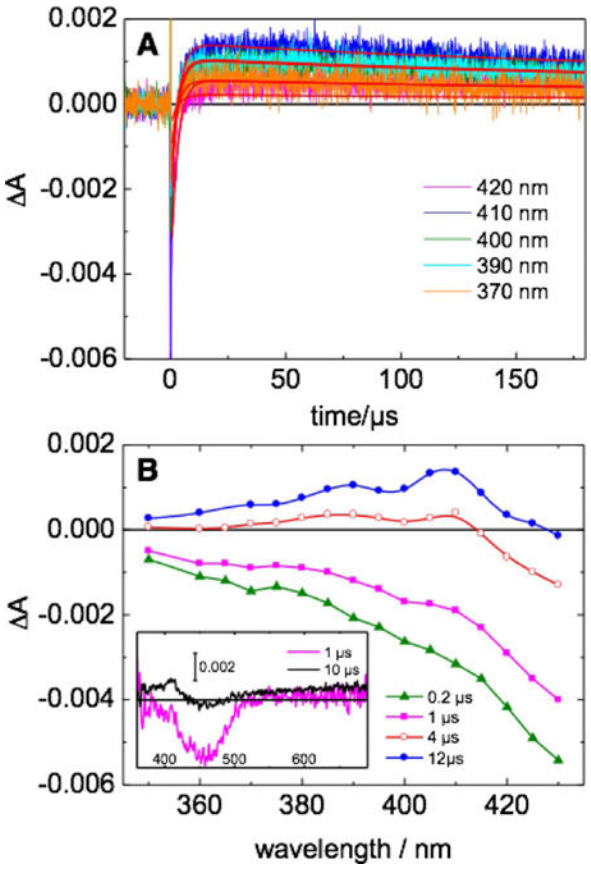

Figure 2.

A) Kinetic traces at different wavelengths for an argon-purged aqueous solution of α_3DH_3-**Rubpymal** in the presence of 20 mM $[Ru^{III}(NH_3)_6]^{3+}$, 20 mM acetate-phosphate-borate (APB), 140 mM KCl, pH 5.0. Excitation at λ = 460 nm, laser energy 4 mJ. Red curves correspond to global fitting analysis. B) Differential absorption spectrum calculated from kinetic traces in (A). The spectrum of the tyrosine radical is observed at 12 μs post-laser flash. Inset in (B): transient absorption spectra from 350–700nm.

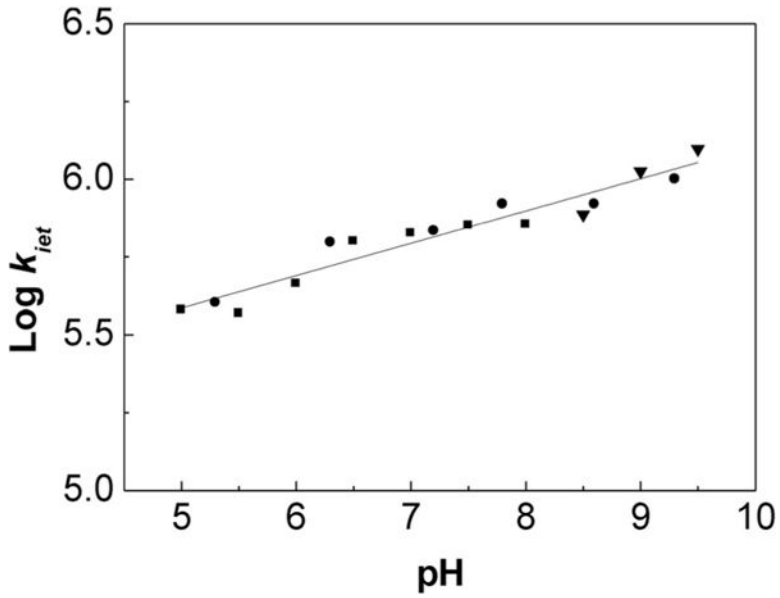

Figure 3.
The pH dependence of k_{iet} values from pH 5 to 9.5 in 20 mM APB buffer with 140 mM KCl.

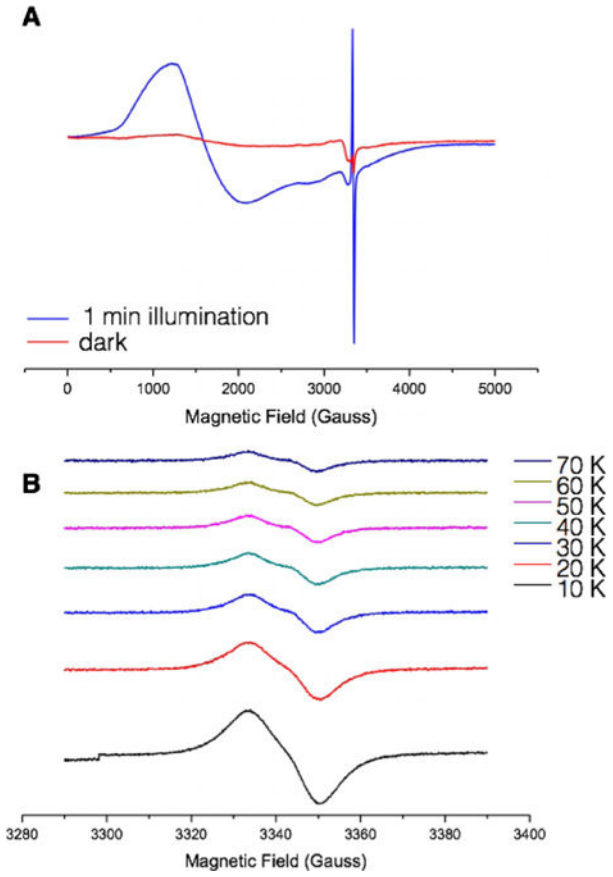

Figure 4.

A) EPR spectra of α_3DH_3-**Rubpymal** in the dark (red trace) and after exposure to light at 460 nm for 1 min (blue trace). Conditions: 0.17 mM α_3DH_3-**Rubpymal**, 7.2 mM $[Co^{III}(NH_3)_5Cl]^{2+}$, pH 5.5, temperature 10 K, microwave frequency 9.38 GHz, microwave power 0.04 mW, modulation amplitude 10 G, modulation frequency 100 kHz. B) EPR spectra of tyrosyl radical in α_3DH_3-**Rubpymal** from 10 K to 70 K. Conditions: as for (A) but with a modulation amplitude of 2 G.

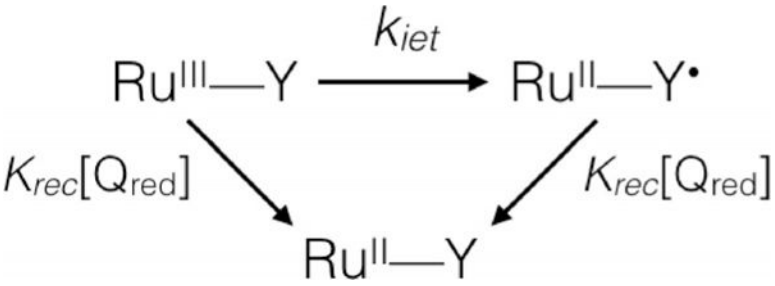

Scheme 1.
Reaction model for global fitting analysis.